JOURNAL OF AIRCRAFT
Vol. 46, No. 6, November–December 2009

Parametric Study of an Axisymmetric Busemann Biplane Configuration

Dan Igra* and Eran Arad†
Rafael Advanced Defense Systems, Ltd., Haifa 31021, Israel

DOI: 10.2514/1.41472

The axisymmetric Busemann biplane was investigated numerically. This configuration is composed of two cylindrical wings for which the cross section was similar to a regular two-dimensional Busemann biplane. The influence of various flow conditions on the drag coefficient was investigated. The axisymmetric configuration was found to be less effective than a two-dimensional Busemann biplane. However, drag was significantly smaller than that of a single-wing shape.

Nomenclature

A_{ref} = reference area
c = wing chord length, m
c_D = drag coefficient
h = minimum distance between the wings, m
M_D = design Mach number
M_s = solution Mach number
R = distance between the symmetry line and the bottom wing, m
θ = wedge angle, deg

I. Introduction

THE Busemann biplane is an apparatus that reduces the wave drag of a particular geometry at supersonic speeds. This geometry was first suggested by Busemann [1] in 1935. It is composed of two wedge-shaped wings facing each other. These wings are designed to reduce the wave drag by creating a wave system that is confined between the two wings. To achieve this flow structure, the distance between the two wings is set as a function of the free flow Mach number. Over the years, the Busemann biplane was investigated by many researchers. Some experimental results have been reported in [2,3]. In recent years, there has been a renewed interest in Busemann biplane configuration. Some, such as [4,5], have shown interest in aerodynamic design, and others, such as [6], have applied this configuration to a scramjet engine. Previously [5], we conducted a parametric study of the two-dimensional Busemann biplane phenomena using numerical simulation. In the present study, we have extended the scope to an axisymmetric Busemann biplane.

Hoerner [3] discussed an axisymmetric Busemann biplane configuration that consists of a shrouded body, shown in Fig. 1. A similar configuration was discussed by Ferri [7] as well. This configuration consists of a ring positioned around the body in a manner that causes the shock waves to be captured between the ring and body. However, the implementation of this configuration is difficult for existing aeronautical designs. Therefore, we suggest a new approach here. It is composed of two rings that have a cross section similar to that of the two-dimensional Busemann biplane shown in Fig. 2. The main advantage of this new setup over existing Busemann biplane configurations is that the two-ring geometry is much easier to incorporate into existing configurations. One possible use of this design is reduction of base drag in supersonic flow. The double-ring set can be positioned so that it increases base pressure and thereby decreases the base drag. Drag reduction in a Busemann biplane occurs only when uniform pressure distribution over the two facing wings is developed. Originally, the constant pressure was approximated using a linearized theory in which shock waves and expansion waves are of minute thickness. This analysis was presented in previous works such as [2]. While this is a good approximation for shock waves, expansion waves by nature are expanding and therefore occupy some space.

Consequently, a nonuniform pressure profile develops over wings that were designed using this approximation, and additional drag is generated. To define a more accurate model of the problem, a numerical simulation was conducted in [5] to study the flow over a two-dimensional Busemann biplane configuration. It was found that a properly designed configuration has a lower drag coefficient than that of single wedge-shaped wing. In addition, as the design Mach number grows higher, the Busemann biplane is less sensitive to variation in the flow velocity or angle of attack. In the current phase, we have studied the performance of an axisymmetric Busemann biplane configuration. The analysis focused on the following aspects: 1) influence of the radius on the drag coefficient, 2) performance at offdesign conditions, and 3) effect of turbulent flow conditions on performance.

II. Computation Setup and Numerical Method

The configuration employed in the present work is shown in Fig. 2. The profile had a front wedge angle θ of 10 deg and a chord length c of 0.2 m. The radius-to-chord ratio R/c varied from 0.35 to 7.5. The biplane was designed for two Mach numbers: $M_D = 2$ and 3. It is the design Mach number that sets the distance between the two wings (or rings). This constraint is dictated by the requirement that the shock wave that commences at the leading edge of each wing should hit the other wing exactly at its maximum thickness location. From this location, the expansion wave unfolds. All flow conditions in the numerical simulation are for standard atmosphere air at sea level.

The reference area used in the drag coefficient calculation is πR^2. The computations for the zero-angle-of-attack case were performed using a two-dimensional axisymmetric flow domain. The flow domain contains two wedgelike wings, and below them is the symmetry axis, as shown in Fig. 2. On the other boundaries, uniform flow conditions were defined. The solution domain and boundary conditions are presented in Fig. 3. The computational mesh was generated using the ICEM CFD [8] mesh generator and is shown in Figs. 4 and 5. The inflow boundary is located $4c$ from the biplane, the outflow boundary is $10c$ downstream of the biplane, and the top boundary is located about $7c$ above the biplane.

The axisymmetric two-dimensional mesh presented in Fig. 4 consists of 46,004 cells that are clustered at the shock wave locations

Presented as Paper 3726 at the 38th Fluid Dynamics Conference and Exhibit, Seattle, WA, 23–26 June 2008; received 8 October 2008; revision received 21 July 2009; accepted for publication 31 July 2009.

*Senior Staff Scientist.
†Head of Computational Fluid Dynamics Group.

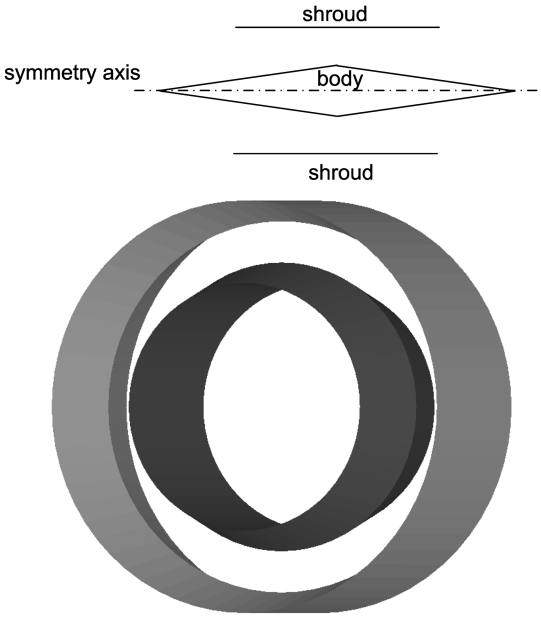

Fig. 1 Configuration of Hoerner [3] axisymmetric Busemann biplane.

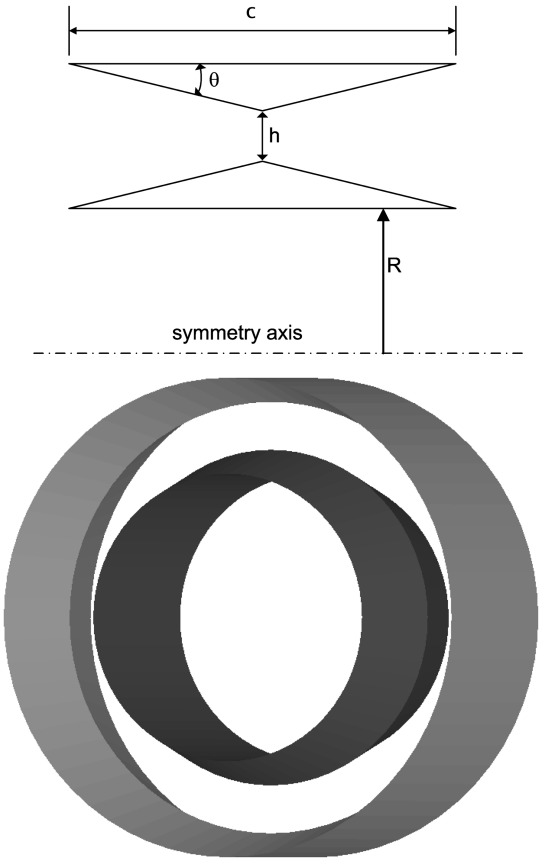

Fig. 2 Configuration of the two-ring axisymmetric Busemann biplane.

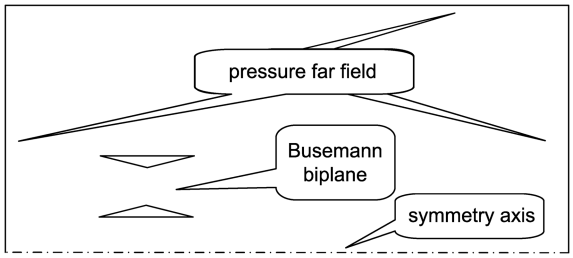

Fig. 3 Flow domain and boundary conditions.

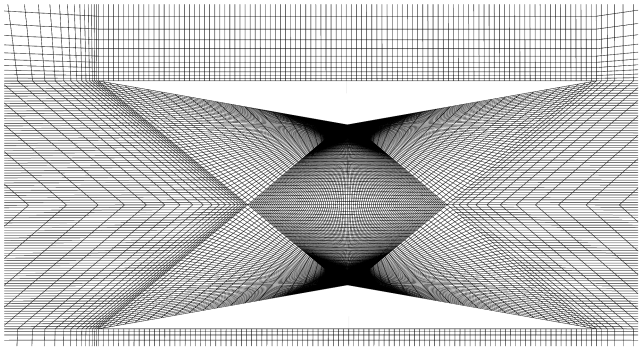

Fig. 4 Computational mesh for two-dimensional axisymmetric flow domain.

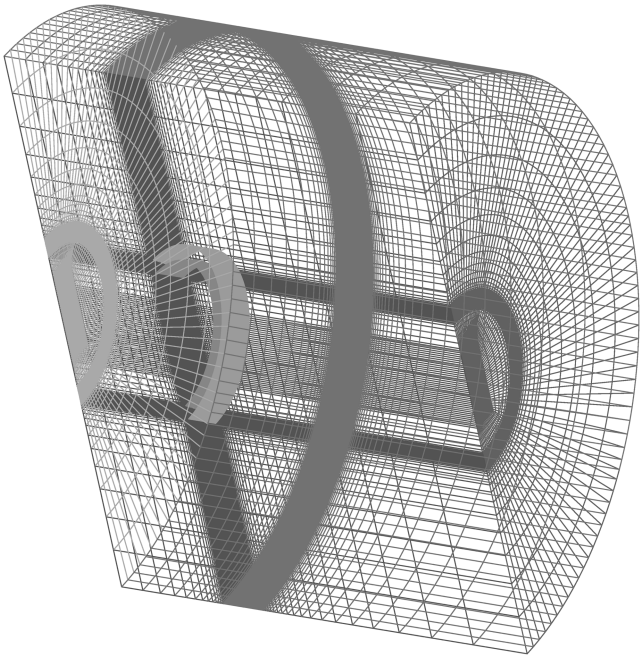

Fig. 5 Computational mesh for three-dimensional flow domain.

between the two wings. The mesh was designed for proper shock wave resolution using an inviscid solver. Within this concept, the relatively coarse mesh on the exterior part of the set (Fig. 4) has no influence on the results. For calculations of the non-zero-angle-of-attack cases, a three-dimensional configuration was produced by rotating the original two-dimensional model by 180 deg. Thus, one-half of the entire flow domain was created using a symmetry plane as a boundary. Although the mesh for this flowfield is based on that of the two-dimensional mesh, it is still coarser. The three-dimensional mesh contains about 1.7 million cells over one-half configuration and is shown in Fig. 5. This mesh was constructed so that at zero angle of attack it would produce a drag similar to that of the two-dimensional axisymmetric solution.

The computations were carried out using FLUENT 6 [9] code. Most of the computations were performed using a compressible inviscid flow model, solving the Euler equations. The solutions for turbulent flow were carried out using the standard k-ε turbulence model with nonequilibrium wall functions. For these flow computations, a new mesh was created that was suitable for turbulent flow. Significant increase in mesh size was not required. However, the mesh cells were clustered toward the wing to reach a maximal value of $Y_+ = 150$. The results of the grid sensitivity analysis and grid convergence are discussed in Appendix A. Further validation of the

present results would have been a comparison with the experiments' results. However, measurements for a rotational biwing configuration are not presently available (to the best knowledge of the authors). Comparison of the computed results with analytical solution is an alternative venue for validation. However, such an analytical approach is feasible only for 2-D geometry, where oblique shock wave and expansion fans theory can be used to compute the drag coefficient. Thus, the results of our previous study [5] (2-D Busemann biplane solved using the same FLUENT 6 [9] solver) are compared herein with the analytical solution. For a design Mach number 3, the analytical value of the drag coefficient is 0.0026, whereas in [5] the numerical simulation resulted in a value of 0.00257.

III. Computational Results

A. Flowfield Analysis

The pressure contours around an axisymmetric Busemann biplane with $R/c = 2.5$ and design Mach number $M_D = 2$ are shown in Fig. 6. The shock waves are reflected from the wing's leading edges interact with each other and then reflect back toward the opposing wing. The reflected waves reach the thickest section of each wing. From this position the flow cross section increases downstream producing expansion waves. These expansion waves propagate toward each other and reflect back toward the wings trailing edges. Figure 6 clearly demonstrates that the shock waves are confined within the wings (rings) of this configuration. This is the requirement for the reduction of the drag force. The shock waves at the top and bottom of the axisymmetric configuration have different shapes due to the axisymmetric nature of the flowfield. In this way, the present application differs from the two-dimensional Busemann biplane, for which the two shock waves are identical. The pressure contours for $R/c = 2.5$ and design Mach number 3 flow are shown in Fig. 7. For the higher Mach number, the distance between the wings is about one-half of the previous one. Here, too, the waves are confined within the two-rings set.

As can be expected the maximum pressure in the Mach 3 flow is higher than that in the Mach 2 flow, although the location of the maximum pressure region is similar. It is located on the upper tip of the bottom wing. In addition, for the higher Mach number, the shock deflection angle is smaller than that of the Mach 2 case.

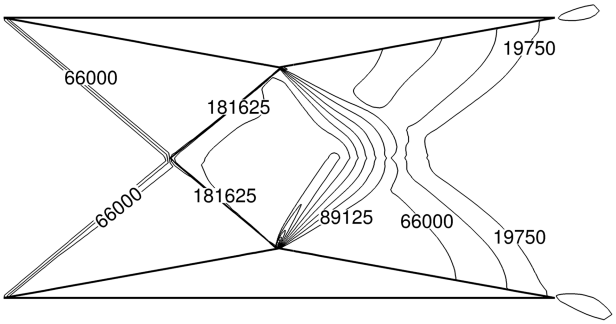

Fig. 6 Pressure contours $p - p_\infty$ (Pa) around an axisymmetric Busemann biplane. Flow at design Mach number 2, zero angle of attack, and $R/c = 2.5$.

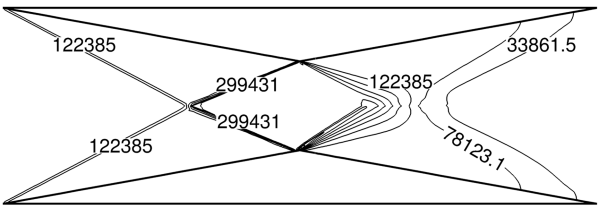

Fig. 7 Pressure contours $p - p_\infty$ (Pa) around an axisymmetric Busemann biplane. Flow at design Mach number 3, zero angle of attack, and $R/c = 2.5$.

B. Influence of the Configuration Radius on the Drag

The effect of the internal radius on the drag was evaluated in a parametric study. Computations were performed for Mach numbers 2 and 3. The distance between the rings depends on the design Mach number. Thus,

$$\left.\frac{h}{c}\right|_{M_D=2} = 0.32, \qquad \left.\frac{h}{c}\right|_{M_D=3} = 0.15$$

Figure 8 shows the drag coefficient for two Mach numbers versus R/c (nondimensional radius). It can be seen that as the ratio R/c increases, the drag coefficient decreases. Initially, a slight decrease in R/c results in a large decrease in the drag coefficient. However, above $R/c = 2$ the improvement in the drag coefficient is less significant. The drag coefficient for Mach 3 is lower than that of Mach 2. Figure 9 displays the drag coefficient vs R/h. The drag coefficient varies inversely with the ratio R/h. It appears that for values of R/h larger than 10, further decrease in the drag coefficient is incremental. It should be noted here that for each Mach number, a single optimal value of h is used and R is modified. Since the gap between the wings for Mach 3 is about one-half of that used for Mach 2, Fig. 9 is somehow misleading: For each radius R, the drag coefficient computed at Mach 3 is smaller than that computed at Mach 2. Out of these results one can draw a correlation for the drag dependence on both nondimensional parameters: R/c and R/h.

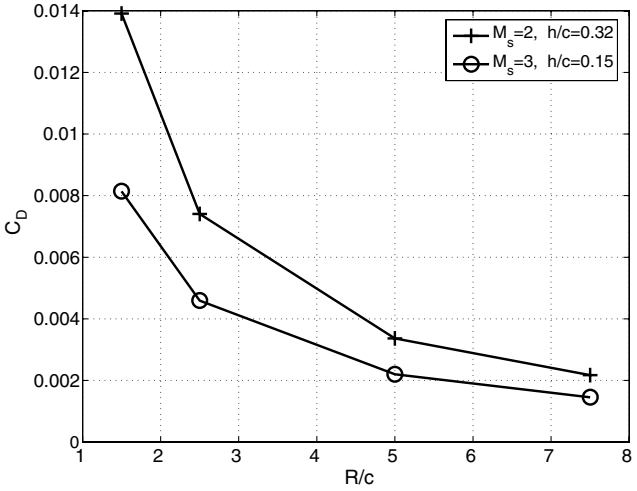

Fig. 8 Drag coefficient vs R/c for two Mach numbers based on reference area $A_{\text{ref}} = \pi R^2$.

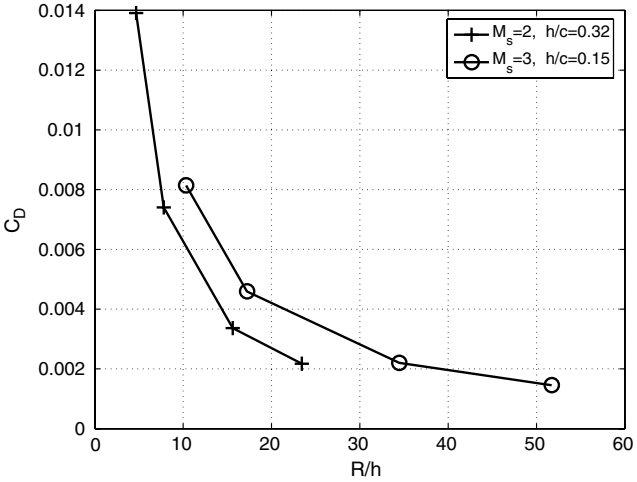

Fig. 9 Drag coefficient vs R/h for two Mach numbers based on reference area $A_{\text{ref}} = \pi R^2$.

The analysis presented above was done using a reference area of πR^2, which is the most obvious choice for axisymmetric geometry. However, one might argue that the area between the two wings is a more suitable reference area, since as $R \to \infty$, the aerodynamic coefficients approach the 2-D value. That way, the effect of the rotational geometry can be clearly identified. The alternative reference area has a ring shape with the width of h (see Fig. 2). This ring's area depends on the design Mach number, as h does. Consequently, the reference area for design Mach number 2 is larger than that of design Mach number 3. The Mach-dependent reference area affects the drag coefficients, as shown in Fig. 10: $C_D^{(1)}$ for design Mach number 2 is lower than that of design Mach number 3 (opposite trend to that identified when a uniform reference area was used). As R increases, both curves appear to flatten and reach a constant value. As R approaches infinity, the drag coefficients of the axisymmetric configuration approach that of a two-dimensional case [5], in which the drag coefficient was 0.0243 and 0.0345 for design Mach numbers 2 and 3, respectively. The drag coefficient in the 2-D case was also calculated using the area between the wings as a reference area.

Naturally, the drag of the axisymmetric Busemann biplane should be compared with that of a single ring. Such a comparison for Mach numbers 2 and 3 is presented in Figs. 11 and 12, respectively. The single wing has a ring shape with a wedge cross section, as shown in Fig. 13. In these figures there are two types of single-wing geometries. Single wing *i* refers to a cylinder-shaped wing for which the wedge is directed toward the symmetry axis. Single wing *e* refers to a cylinder with a uniform internal diameter. However, it was found out that the single wings have a similar drag (see Figs. 11 and 12). Therefore, in the following sections only one single-wing configuration will be used for comparison. Figures 11 and 12 show that the axisymmetric Busemann biplane reduces the drag coefficient by a factor of 4. This reduction is smaller than that obtained for a two-dimensional Busemann biplane [5] where the drag coefficient was reduced by one order of magnitude.

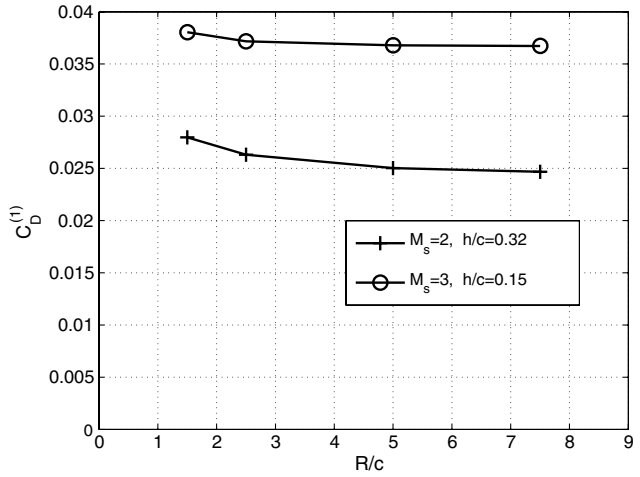

Fig. 10 Drag coefficient vs R/c for two Mach numbers based on reference area $A(h, R)$.

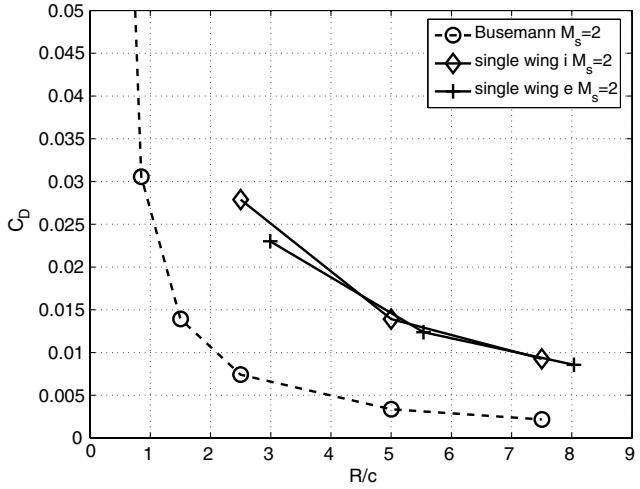

Fig. 11 Drag coefficient comparison of an axisymmetric Busemann biplane with a single ring ($M_D = 2$).

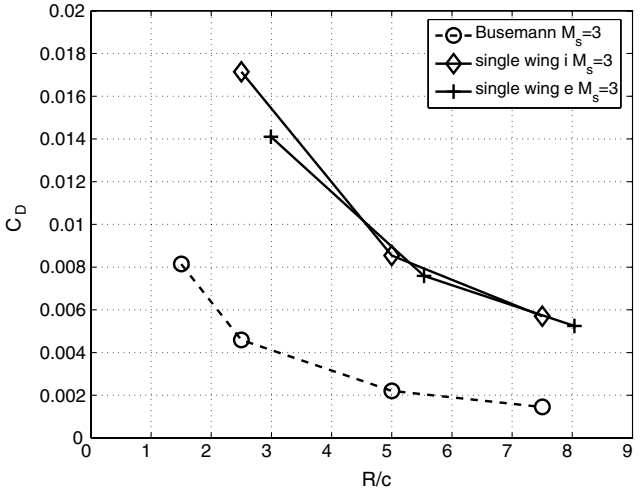

Fig. 12 Drag coefficient comparison of an axisymmetric Busemann biplane with a single ring ($M_D = 3$).

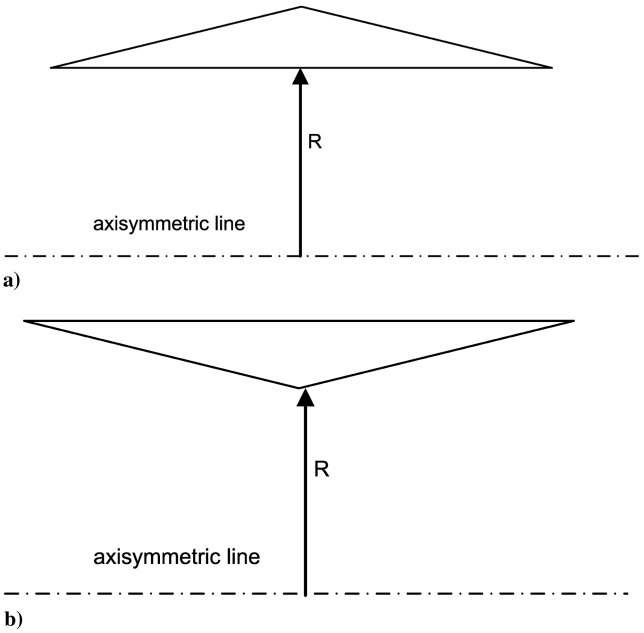

Fig. 13 Configurations of a) single wing *i* and b) single wing *e*.

C. Offdesign Performance

Although this biplane provides a significant reduction of drag at the design point, its performance depends on accurate positioning of the wings and the locations of the shock waves. Therefore, from a practical point of view, the analysis of the performance at offdesign situations is crucial. For a two-dimensional biplane [5], it was found that offdesign flow Mach numbers affect the drag and, in some cases, produced a drag that is greater than that of a single wing. The axisymmetric configurations that were designed for Mach numbers of 2 and 3 were subjected to a flow with Mach numbers ranging from 1.9 to 4, as shown in Figs. 14 and 15 respectively. The results are compared to the drag coefficient of a single wedge wing under similar flow conditions. It can be seen that when the flow Mach number is

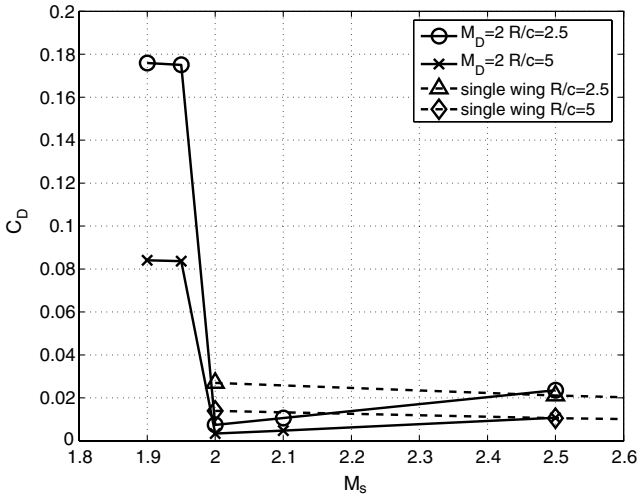

Fig. 14 Drag coefficient vs flow Mach number for design Mach number 2.

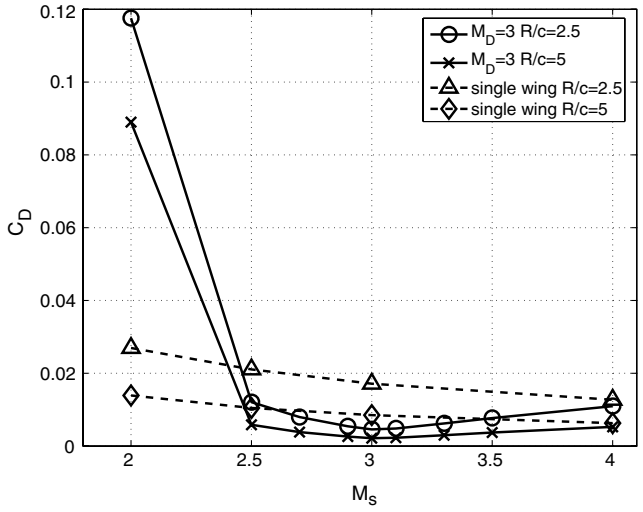

Fig. 15 Drag coefficient vs flow Mach number for design Mach number 3.

larger than the design Mach number, the drag coefficient is increasing at a low rate and is still much lower than the drag coefficient of a single wing. However, when the flow Mach number is below the design Mach number, a sudden increase in the drag coefficient is observed and it becomes larger than that of a single wing. This behavior is due to the fact that shock waves are no longer confined between the rings. In such a case, a detached shock wave develops, as shown in Fig. 16 for the case of a design Mach number of 2 at a flow Mach number of 1.95. The detached shock wave is positioned in front of the axisymmetric Busemann biplane and produces a high drag coefficient.

It can be seen that for a higher design Mach number, the configuration yields a lower drag coefficient. Thus, the higher the design Mach number of the configuration, the less sensitive it is to changes in the flow Mach number. The region of effectiveness for design Mach number 2 configuration is between Mach numbers 2 and 2.4, whereas that of design Mach number 3 has a much larger effectiveness range from Mach numbers 2.5 to 4. Qualitatively, the results shown in Figs. 14 and 15 are similar to the results of two-dimensional Busemann biplane [5].

It is well known that the structure of shock waves between wedges may be nonunique. A hysteresis phenomenon was observed both experimentally and numerically by Li et al. [10] and others. However, such a trend cannot be identified by the present steady-state flow solution. A time-accurate solution is required to identify the

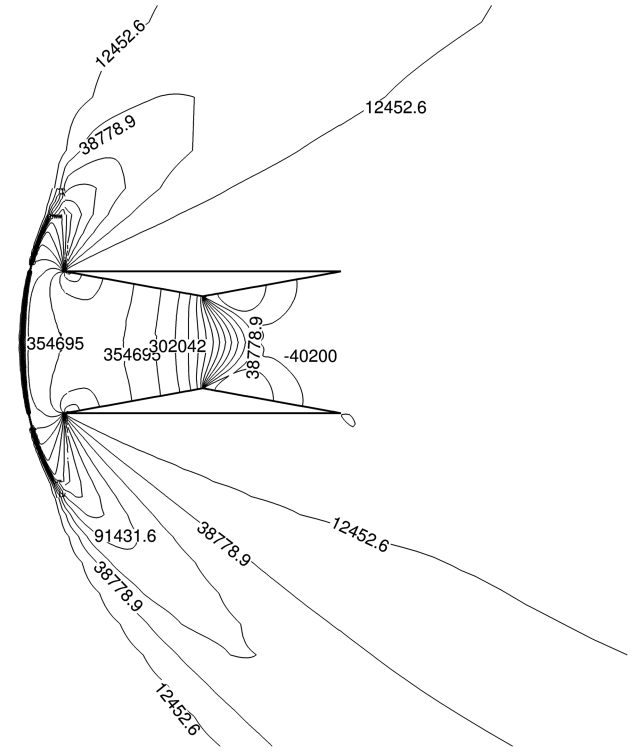

Fig. 16 Pressure contours $p - p_\infty$ (Pa) for $R/c = 2.5$, $M_D = 2$, and $M_s = 1.95$.

nonuniqueness of the flowfield, where different solutions are obtained for a given set of conditions, when Mach increases or decreases. This is an obvious course for further investigation of the present configuration.

D. Effect of Viscous/Turbulent Flow

The Busemann biplane concept was based on inviscid analysis. It is of interest to investigate how this device performs in turbulent flow. The turbulent mechanism may be regarded as an offdesign condition, as it affects the shock wave location. A standard k-ε turbulence model with nonequilibrium wall functions was employed. The drag coefficient for design Mach numbers 2 and 3 is shown in Figs. 17 and 18, respectively. The plots also show a comparison of the drag reduction with inviscid flow. In turbulent flow the drag reduction by the axisymmetric Busemann biplane is almost one-half of that obtained by the inviscid flow model. However, it is still much lower than that of a single wing in turbulent flow conditions.

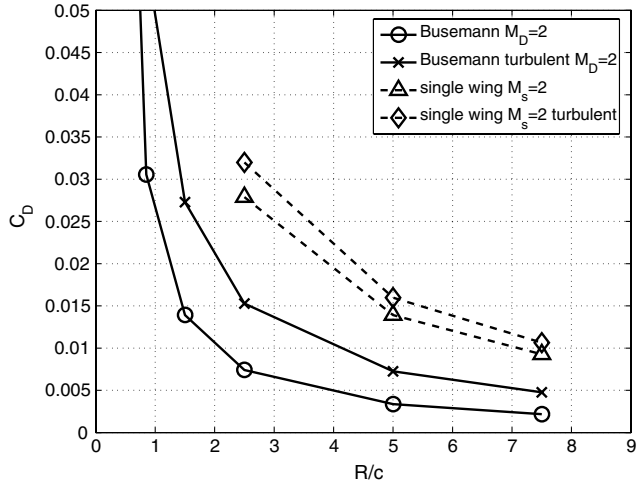

Fig. 17 Drag coefficient vs radius for turbulent flow for $M_D = 2$.

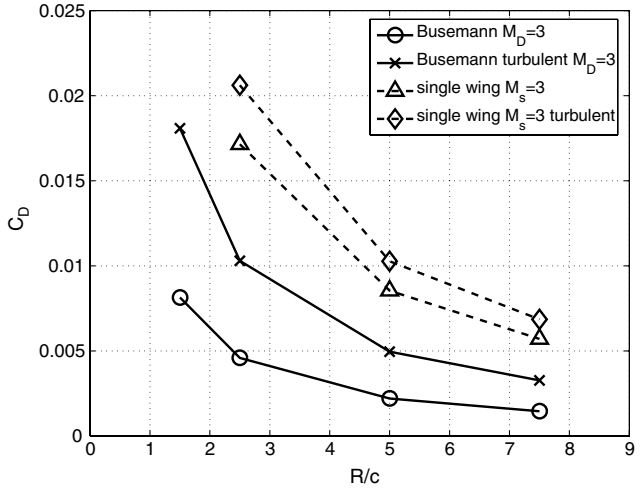

Fig. 18 Drag coefficient vs radius for turbulent flow for $M_D = 3$.

Once again, the results shown in Figs. 17 and 18 are similar qualitatively to those obtained for a two-dimensional Busemann biplane [5]. In both cases, the viscous drag roughly doubles the drag coefficient of both Busemann biplane configurations.

E. Effect of Angle of Attack

This analysis was conducted using three-dimensional computation. For validation, the results obtained for zero angle of attack were compared with the results of the previous section. The difference in the drag coefficient was smaller than 5%. The difference is due to a coarser grid between the rings in the three-dimensional mesh. Employing identical grid distribution for the three-dimensional grids would have resulted in very large grids, whereas we are currently just interested in a comparative study. Thus, the use of a coarser mesh with slightly bigger numerical error is sufficient. Figures 19–22 show the dependence of the drag and lift on angle of attack for two different design Mach numbers. For design Mach number 2 at angles of attack below 2 deg, the drag increases gradually but it is still much lower than that of single wing. Meanwhile, the lift coefficient is slightly higher than that of a single wing. For higher angles of attack, the drag coefficient increases more steeply and becomes larger than that of a single wing, whereas the lift coefficient becomes smaller than that of a single wing. This is the result of a detached shock wave that appears in front of the configuration for these flow conditions, as shown in Fig. 23. For the two-dimensional Busemann biplane under similar

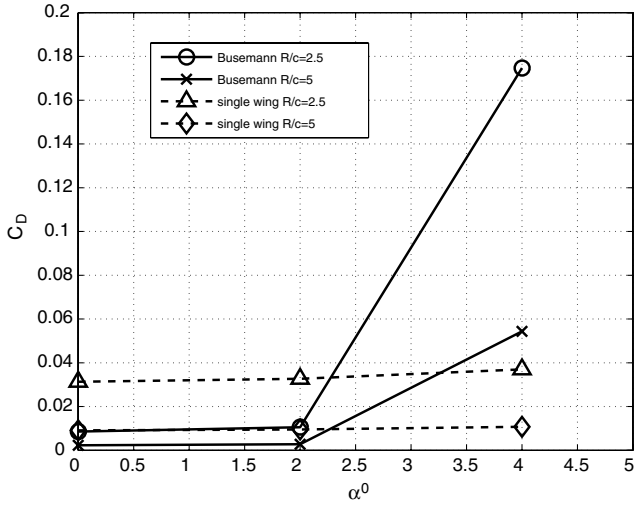

Fig. 19 Drag coefficient vs angle of attack ($M_D = 2$).

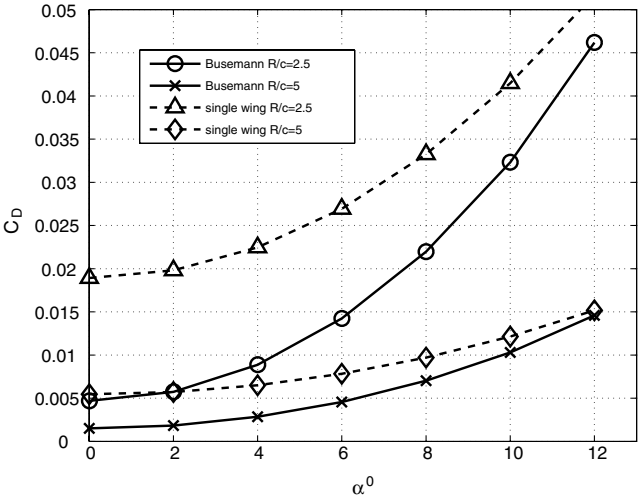

Fig. 20 Drag coefficient vs angle of attack ($M_D = 3$).

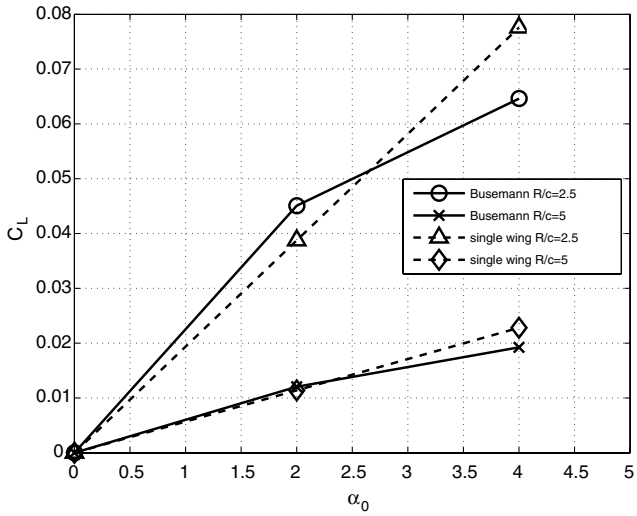

Fig. 21 Lift coefficient vs angle of attack ($M_D = 2$).

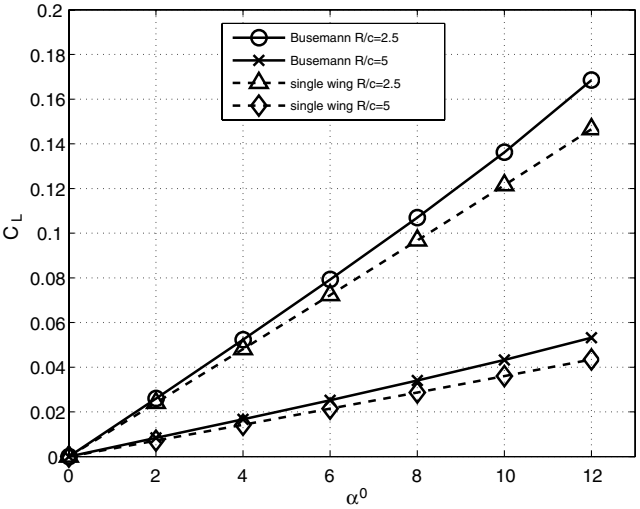

Fig. 22 Lift coefficient vs angle of attack ($M_D = 3$).

flow conditions [5], a detached shock wave appeared for angle of attack larger than 4 deg. In the case of Mach 3 shown in Figs. 20 and 22, increasing the angle of attack gradually increases the drag and lift coefficients. However, for angle of attack lower than 12 deg, the double ring's drag coefficient is still considerably lower than that of a

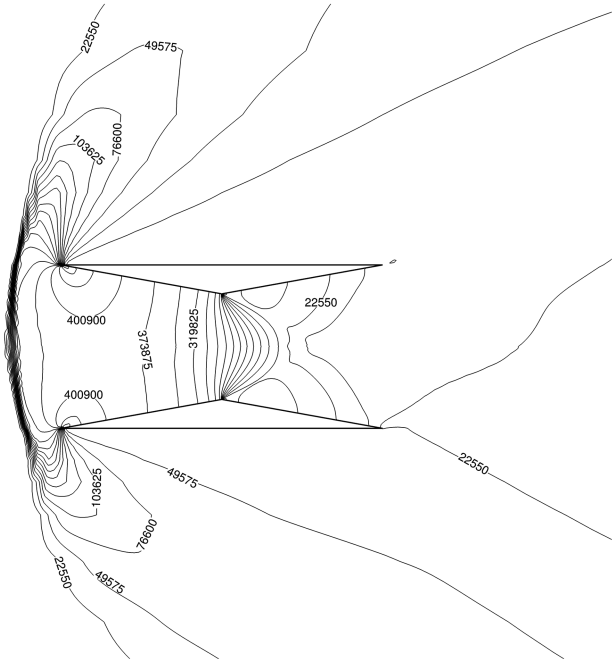

Fig. 23 Pressure contours $p - p_\infty$ (Pa) along symmetry plane for $R/c = 2.5$, $M_D = 2$, and angle of attack of 4 deg.

single wing, whereas the lift coefficient is higher. The same trend was observed for the two-dimensional Busemann biplane under similar flow conditions [5].

IV. Conclusions

The axisymmetric Busemann biplane was investigated numerically. Several performance aspects were studied to find out how they affect the drag coefficient under various flow conditions. It appears that increasing the internal radius reduces the drag coefficient. Under most flow conditions it was found that the axisymmetric Busemann biplane has a lower drag coefficient than that of single cylindrical wedge wing. It was found that configurations that were designed for a higher design Mach number are less sensitive to variation in the flow velocity or angle of attack. The behavior of the current axisymmetric configuration was found to be quite similar to that of a two-dimensional configuration, as reported in [5]. This is true for offdesign Mach number flow and angles of attack.

The present study indicates that from a practical point of view, the biplane configuration is more attractive as the design Mach number grows higher.

Appendix A: Grid Dependence and Convergence Analysis

For the two-dimensional axisymmetric case, a grid sensitivity test was conducted. The results are presented in Fig. A1. The grid size ranged from 13,524 to 136,308 cells. It can be seen in Fig. A1 that the drag coefficient hardly changes once the grid size exceeds 44,000 cells. Consequently, the grid with 46,004 cells was employed for the calculations. Residual convergence plots for two- and three-dimensional flow domains are shown in Figs. A2 and A3 respectively. It can be seen that all equations converge well and the residuals reduce by six orders of magnitude.

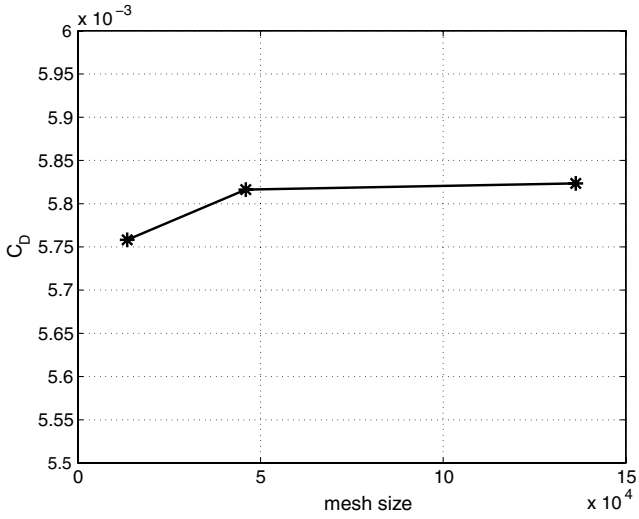

Fig. A1 Grid sensitivity test for the two-dimensional axisymmetric case.

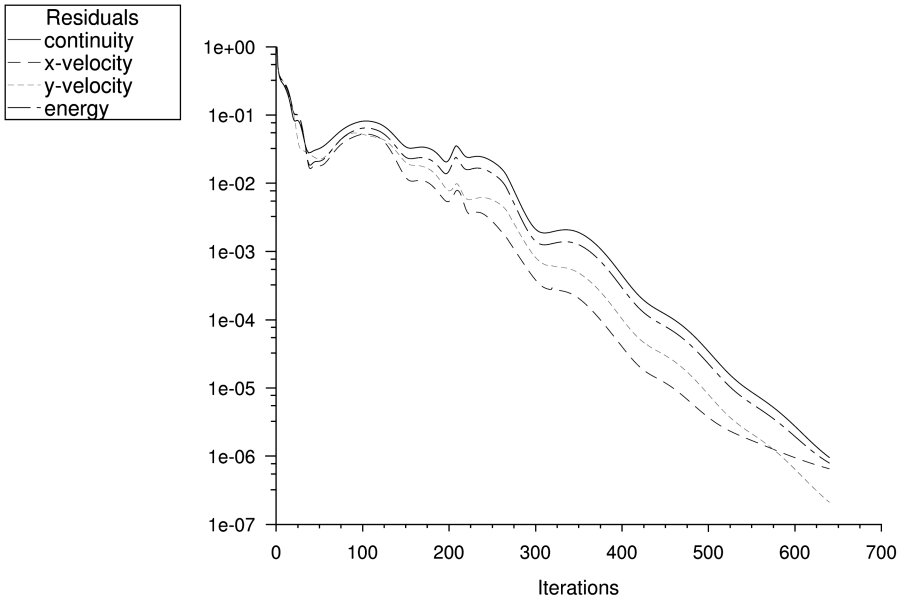

Fig. A2 Convergence monitoring of the solution for a two-dimensional flow domain with 46,004 cells; design Mach number 2 at Mach 2 flow; $R = 0.3$ m; and $R/c = 1.5$.

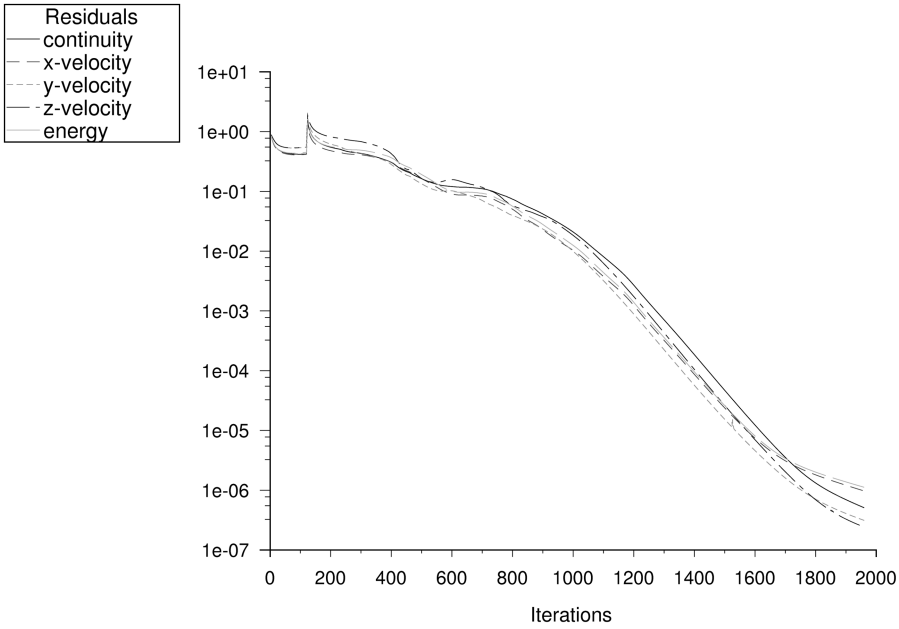

Fig. A3 Convergence monitoring of the solution, for a three-dimensional flow domain with 1.7 million cells; design Mach number 3 at Mach 3 flow; $R = 1.5$ m; and $R/c = 7.5$.

References

[1] Busemann, A., "Aerodynamischer Auftrieb bei Uberschal geschwindigkeit," *Luftfahrt-Forsch*, Vol. 12, 1935, pp. 210–220.

[2] Liepmann, H. W., and Roshko, A., *Elements in Gas Dynamics*, Wiley, New York, 1957, pp. 115–118.

[3] Hoerner, S. F., *Fluid-Dynamic Drag*, published by the author, Midland Park, NJ, 1965, pp. 16–35.

[4] Kusunose, K., Matsushima, K., Goto, Y., Yamashita, H., Yonezawa, M., Maruyama, D., and Nakano, T., "A Fundamental Study for the Development of Boomless Supersonic Transport Aircraft," AIAA Paper 2006-654, 2006.

[5] Igra, D., and Arad, E., "A Parametric Study of the Busemann Biplane Phenomena," *Shock Waves*, Vol. 16, No. 3, 2007, pp. 269–273. doi:10.1007/s00193-006-0070-x

[6] Stalker, R. J., "Waves and Thermodynamics in High Mach Number Propulsive Ducts," *High-Speed Flight Propulsion Systems*, AIAA, Washington, D.C., 1991, pp. 237–264.

[7] Ferri, A., "Application of the Method of Characteristics to Supersonic Rotational Flow," NACA Rept. 841, 1946.

[8] *ICEMCFD v4.3.1 User Manual*,ANSYS, Inc., Canonsburg, PA, 2003.

[9] *FLUENT v.6.1 User Manual*, Fluent, Inc., Lebanon, NH, 2003.

[10] Li, H., Chpoun, A., and Ben-Dor, G., "Reflection of Asymmetric Shock Waves in Steady Flows: Analytical and Experimental Investigations," *22nd International Symposium on Shock Waves*, Univ. of Southampton, Paper 0134, 1999.